applied sciences

MDPI

Article

Evaluation of the Aerodynamic Effect of a Smooth Rounded Roof on Crosswind Stability of a Train by Wind Tunnel Tests

Carlos Esteban Araya Reyes *, Elia Brambilla and Gisella Tomasini *

Department of Mechanical Engineering, Politecnico di Milano, 20156 Milan, Italy
* Correspondence: carlosesteban.araya@polimi.it (C.E.A.R.); gisella.tomasini@polimi.it (G.T.)

Abstract: The advent of high-speed trains led to new issues and constraints for railway network manufacturers and operators. This is the case of crosswind effect, that occurs when train is running in strong wind conditions. The combination of train speed and wind speed generates a relative flow that affects the train stability. Wind tunnel tests on still railway vehicles (relative wind-train velocity in coincidence with absolute wind velocity) are mandatory according to Technical Specification for Interoperability (TSI) to ensure high-speed train safety. However, issues related to the correct evaluation of the full-scale aerodynamic behaviour of the trains can arise. In the present work, aerodynamic force and pressure coefficients measured in wind tunnel tests on a scaled model of ETR1000 high-speed train on single track ballast and rails are presented. The tests were performed in the GVPM wind tunnel of Politecnico di Milano. Results show that different flow behaviours can occur at high yaw angles when the train behaves like a bluff body depending on wind speed used during the test.

Keywords: high-speed trains; wind tunnel tests; train aerodynamics; crosswind; force aerodynamic coefficients; pressure aerodynamic coefficients

Citation: Araya Reyes, C.E.; Brambilla, E.; Tomasini, G. Evaluation of the Aerodynamic Effect of a Smooth Rounded Roof on Crosswind Stability of a Train by Wind Tunnel Tests. *Appl. Sci.* **2023**, *13*, 232. https://doi.org/10.3390/app13010232

Academic Editor: Hassan Hemida

Received: 29 November 2022
Revised: 16 December 2022
Accepted: 20 December 2022
Published: 24 December 2022

1. Introduction

Vehicles aerodynamics is one of the major industrial concerns, especially because great interest is addressed to side wind effects that affect the safety of both road and rail vehicles.

Because trains are susceptible to run on routes exposed to winds, the operation of railway vehicles under crosswinds is a widely studied item. Crosswind stability creates a huge interest as the speed of trains increases, and weight of rolling stock is reduced. Over the past decades, different methodologies to study the phenomenon of crosswind on rail vehicles and infrastructure have been developed and proposed [1–6], and standards are defined and updated with regularity. In Europe, within the framework of the Technical Specification for Interoperability (TSI) [7] and in the European Standard for crosswind assessment of railway vehicles [8], the evaluation of the safety level in presence of crosswind is mandatory for high-speed trains. All the proposed methodologies, included the European regulations, prescribe wind tunnel tests or CFD calculations as starting point of the methodology to obtain the static force aerodynamic coefficients of the vehicle in the presence of crosswind.

On the other hand, to correctly measure aerodynamic loads by wind tunnel tests/CFD calculations is not an easy task. Baker et al., in Refs. [9,10], compare full-scale experimental coefficients with the corresponding ones measured by wind tunnel tests for different train models: a lower agreement between full scale and wind tunnel tests is found, especially for the lift force.

To ensure that wind tunnel tests are representative of the real full-scale conditions, European regulations define specific requirements on the wind tunnel tests, such as the minimum Reynolds number, maximum allowable blockage ratio, maximum height of the boundary layer profile and of level of turbulence [8]. Anyway, in some specific cases,

even if tests are carried out in agreement with these requirements, results in terms of force coefficients could be significantly different.

The first car of the train is the most affected by crosswind, and it has been observed that the geometry of the nose highly influences the behaviour of the flow over the rest of the wagon [11]. At high yaw angles, high-speed train behaves as a bluff-body: the pressure distribution around the section is mainly governed by the separation point on the upper part of the car body [12,13]. In particular, vehicles having a geometry with a cross section characterised by rounded forms, without sharp edges, show aerodynamic coefficients very sensitive to the flow conditions and, specifically, to the turbulence intensity [14,15]. The marshalling length of the train has been also reported to have an impact on the aerodynamic loads, especially for tail and intermediate cars, but negligible for the head car [16]. In general, even if tests are compliant with European Standard in terms of Re number and turbulence intensity, flow behaviours detected by wind tunnel tests/CFD analysis could be significantly different with respect to that occurs at full-scale conditions and consequently, the evaluated aerodynamic coefficients could not completely be representative of the real situation and may lead to wrong conclusions about the safety of the train.

The target of this paper is to show how, for a specific train, different values for the same coefficient can be measured, due to different positions of the separation point. It will be shown that, depending on the wind speed of the test, two different behaviours for the fluid flow around the body of the train arise and, consequently, aerodynamic loads measured at some specific angles in the two flow conditions are significantly different.

In the following section, the train model and the experimental setup adopted for the wind tunnel tests are described. The first vehicle of the ETR1000 train has been modelled at 1:15 scale and the scenario reproducing the single-track ballast and rail according to EN14067-6 standard has been considered; force and pressure aerodynamic coefficients have been measured by a dynamometric balance and 160 pressure taps. In Section 3, the results are presented. The presence of a dual behaviour is observed depending on the wind speed simulated during the test. The effects observed in terms of force are correlated to those obtained in terms of pressure, and the pressure distribution around the vehicle sections is analysed to determine the location of the flow separation point.

2. Methodology: Wind Tunnel Experimental Tests

In this section, the methodology applied to study the flow around the train under crosswind by means of wind tunnel tests is described.

To study the phenomenon, wind tunnel tests were performed in compliance with the European Standard for crosswind assessment EN14067-6:2018 for high-speed trains and TSI. In this case, the relative wind yaw angle given by a particular combination of train and wind speed, is reproduced in the wind tunnel test by the equivalent case in which the wind velocity acts on the static model of the train with an absolute yaw angle β_w.

The studied vehicle is the Italian ETR1000, the high-speed train of the Italian railway system, operating at the speed of 300 km/h. The train convoy is composed of eight coaches in fixed composition for a length of 202 m. In line with other modern high-speed trains, the cross section of the ETR1000 is characterised by the presence of a closed smooth rounded roof. The train nose, on the contrary, is characterised by the presence of sharp edges. For this study, the first car of the ETR1000 was reproduced in 1:15 scale, and then, to correctly reproduce the boundary conditions, one-half of the second vehicle has been added to the tested model.

Forces and moments are measured by means of a dynamometric balance, rigidly connected to the first vehicle model, while 160 pressure taps are placed on the surface of the scaled model to measure pressure distribution.

Experimental Setup

Wind tunnel tests were performed in the GVPM (Galleria del Vento Politecnico di Milano) wind tunnel of Politecnico di Milano. This facility corresponds to a closed-circuit

wind tunnel with two test sections placed in a vertical arrangement. For this test campaign, the high-speed (characterised by a very low turbulence intensity) test section of the wind tunnel facility was used. The main characteristics of the high-speed test section of wind tunnel are summarised in Table 1.

Table 1. Wind tunnel test section characteristics.

Test Section	Dimensions [m]	Max Wind Speed [m/s]	Turbulence Intensity [%]
GVPM High-speed	4 × 3.84 × 6	55	<0.1

The scaled model was mounted over a splitter plate specifically developed to control the boundary layer thickness. In Figure 1a a picture of the splitter plate mounted in the test section is displayed; while in Figure 1b, the vertical profile of the mean wind speed measured over the splitter plate and the target value required by the EN14067-6 are plotted.

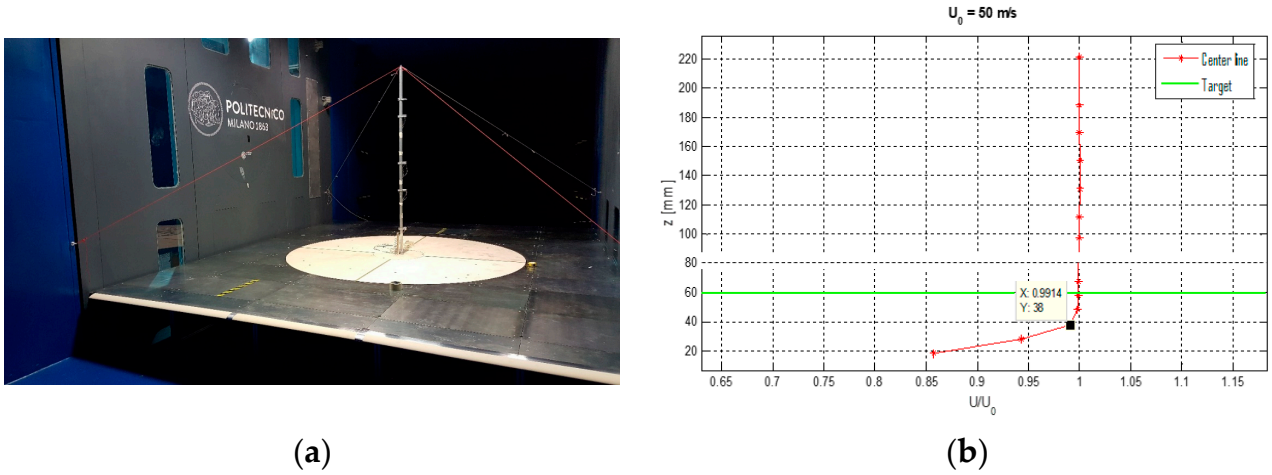

Figure 1. Splitter plate of GVPM wind tunnel: (**a**) Splitter plate mounted on the test section; (**b**) vertical profile of the mean wind speed measured over the splitter plate.

The instrumentation used during the test to measure forces and moments is a six-components dynamometric balance, a strain-gauge based balance (RUAG Aerospace model 19).

The scaled model was instrumented also with pressure sensors. Pressure measurements were performed using the Initium high-speed scanning pressure equipment and the ESP miniature pressure scanners. The small size of the scanners allows them to be positioned inside the model near the measurement points, thus reducing the length of the tubes.

The scaled model of the train consists of:

1. First car: instrumented with an internal six-component dynamometric balance for measuring forces and moments, and 160 pressure taps placed around the surface of the vehicle;
2. Dummy car: placed downstream to reproduce the correct boundary conditions; it corresponds to half of the second vehicle, in compliance with the requirement prescribed by the EN 14067-6 standard.

All the dimensions of the original vehicle were reduced following the 1:15 scale ratio, in order to obtain geometric similarity with the real train. The 1:15 scale ensures the minimum Reynolds number required by the European Standard (2.5×10^5) at both wind speeds is reached.

Mechanical contact between instrumented model (first vehicle) and dummy car is always avoided. The distance between the two vehicles was reproduced with the correct

separation that is present on the real train. The geometry of bogies was simplified in agreement with the EN 14067-6 standard. Infrastructure scenario corresponds to the standard Single Track Ballast and Rails, STBR (EN-14067-6). The wind tunnel scaled model of the ETR1000 train is displayed in Figure 2, on the left: the CAD model of the scaled train and infrastructure scenario is illustrated; on the right: the actual scaled model mounted on the high-speed test section of the wind tunnel is displayed.

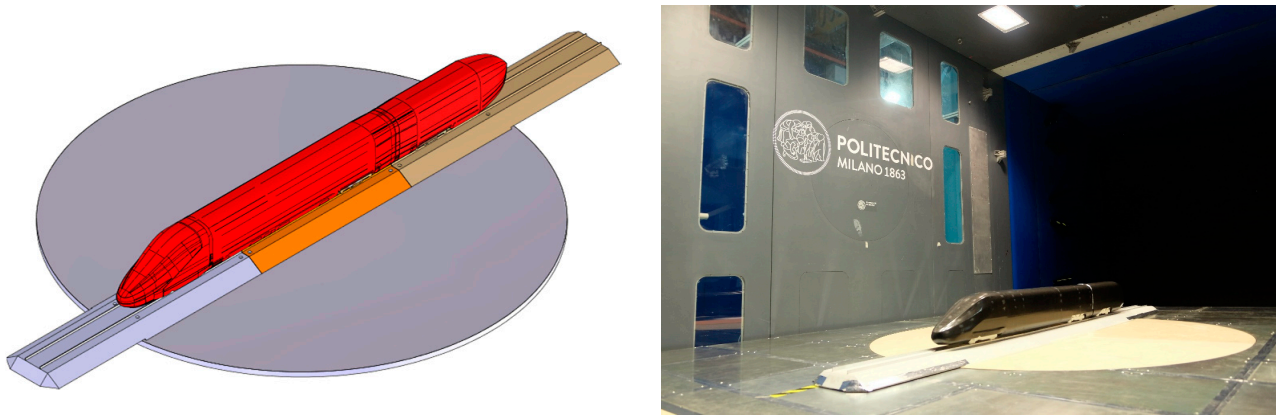

(**a**) (**b**)

Figure 2. Wind tunnel model of ETR1000: (**a**) CAD model; (**b**) scaled model on GVPM wind tunnel.

The dynamometric balance is mounted inside the scaled model, fixed to the car body and to the balance support. This support is rigidly connected to the rotating table of the wind tunnel using two vertical bars placed in correspondence of the bogies as shown in Figure 3.

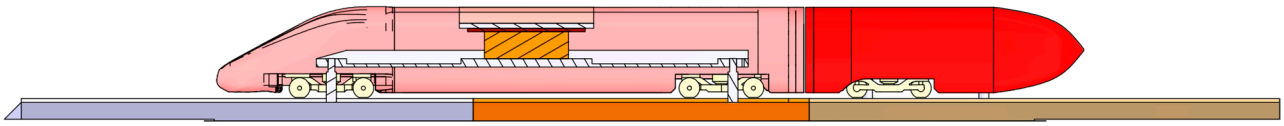

Figure 3. Internal setup for the connection of the dynamometric balance to the train scaled model.

Moreover, to also measure the pressure around the surface of the first car, 160 pressure taps were disposed on the train surface. Eleven rings of pressure taps were set along the train in the positions indicated in Figure 4.

Tests were carried out at two different wind speeds, 30 m/s and 55 m/s. The corresponding Reynolds numbers, calculated with a characteristic dimension of 3 m full-scale as required by EN14067-6, are respectively equal to 4×10^5 and 6.8×10^5, both higher than the limit value of 2.5×10^5 required by the European Standard.

Reference system for evaluating aerodynamic coefficients is defined according to EN14067-6. The reference system is fixed to the vehicle and its origin coincides with the centre of the vehicle at the level of the top of the rail: the longitudinal axis x is oriented in the direction of travel, the z axis is vertical and direct downwards, and the y-axis is perpendicularly oriented to form a right-handed coordinate system. The reference system for computing aerodynamic coefficients is depicted in the Figure 5, where also the yaw angle β_w of the train with respect to the wind direction is represented. $\beta_w = 0°$ when the train is aligned with the wind; β_w is positive if the rotation is clockwise and negative for counter-clockwise rotations.

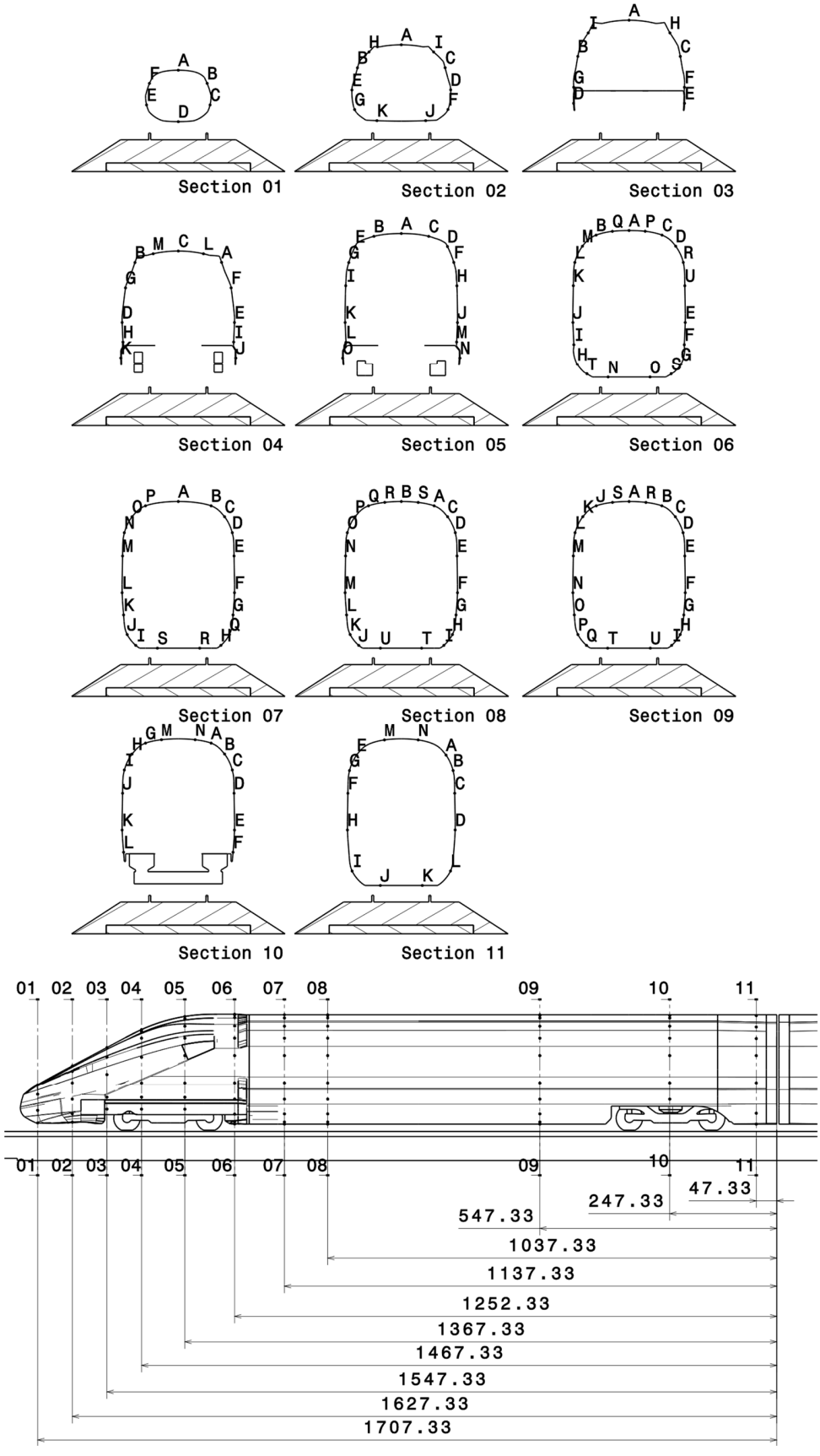

Figure 4. Pressure taps location (quotes in mm).

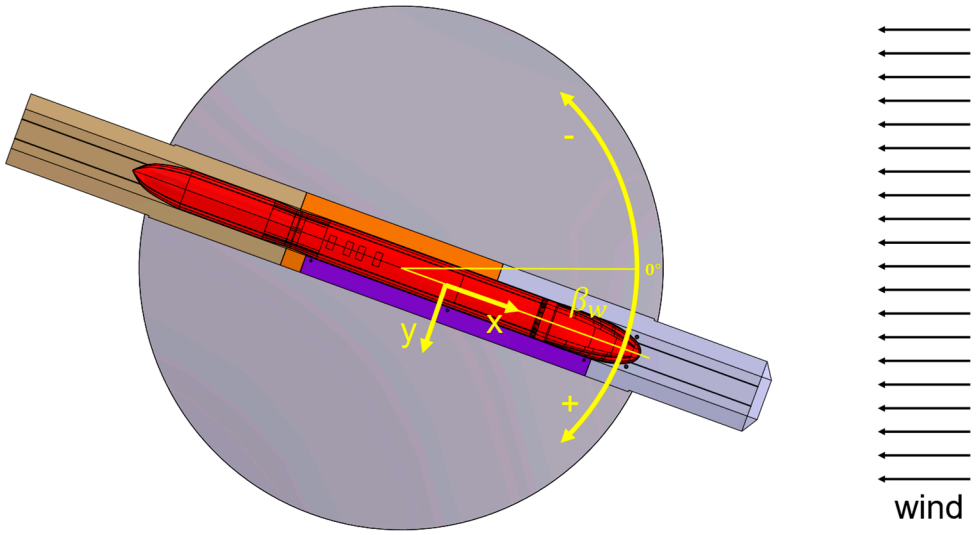

Figure 5. Reference system for wind tunnel test.

From the EN14067-6, aerodynamic coefficients are defined as follow:

$$C_{F_i} = \frac{F_i}{\frac{1}{2}\rho A \overline{U}^2} \quad i = \{x, y, z\} \tag{1}$$

$$C_{M_i} = \frac{M_i}{\frac{1}{2}\rho A h \overline{U}^2} \quad i = \{x, y, z\} \tag{2}$$

$$C_{M_{x,lee}} = \frac{M_x - F_z s}{1/2 \rho A h \overline{U}^2} = C_{M_x} - C_{F_z} \frac{s}{h} \tag{3}$$

where F_i with $i = \{x, y, z\}$ is the force component in the European Standard reference system and M_i is the correspondent moment. In Equations (1)–(3), ρ is the air density, $\overline{U}^2$ is the square of the mean value of wind speed, h is 3 m (at full-scale), A is the reference surface area, defined in the standard as 10 m^2 (full-scale) and s is half of the track gauge (0.75 m for standard gauge according to EN14067-6).

The lee-rail rolling moment corresponds to moment with respect to a longitudinal axis set in accordance with the leeward rail. $C_{Mx,lee}$ is computed from the roll moment coefficient and vertical force coefficient.

3. Results

In this section, the results obtained in the experimental campaign carried out in the wind tunnel of Politecnico di Milano are presented in terms of both force/moment coefficients, computed according to Equations (1)–(3), and pressure coefficient distributions for all the eleven considered sections.

3.1. Aerodynamic Coefficients

Figure 6 shows the four main force coefficients C_{Fy}, C_{Fz}, C_{Mx} and $C_{Mx,lee}$ measured for the ETR1000 train on STBR, for two different wind speeds, 30 m/s and 50 m/s. From the analysis of all the coefficients, it is possible to identify two different trends: over 60°, the curves suddenly separate and then collapse again to similar values at wind yaw angles near 90°.

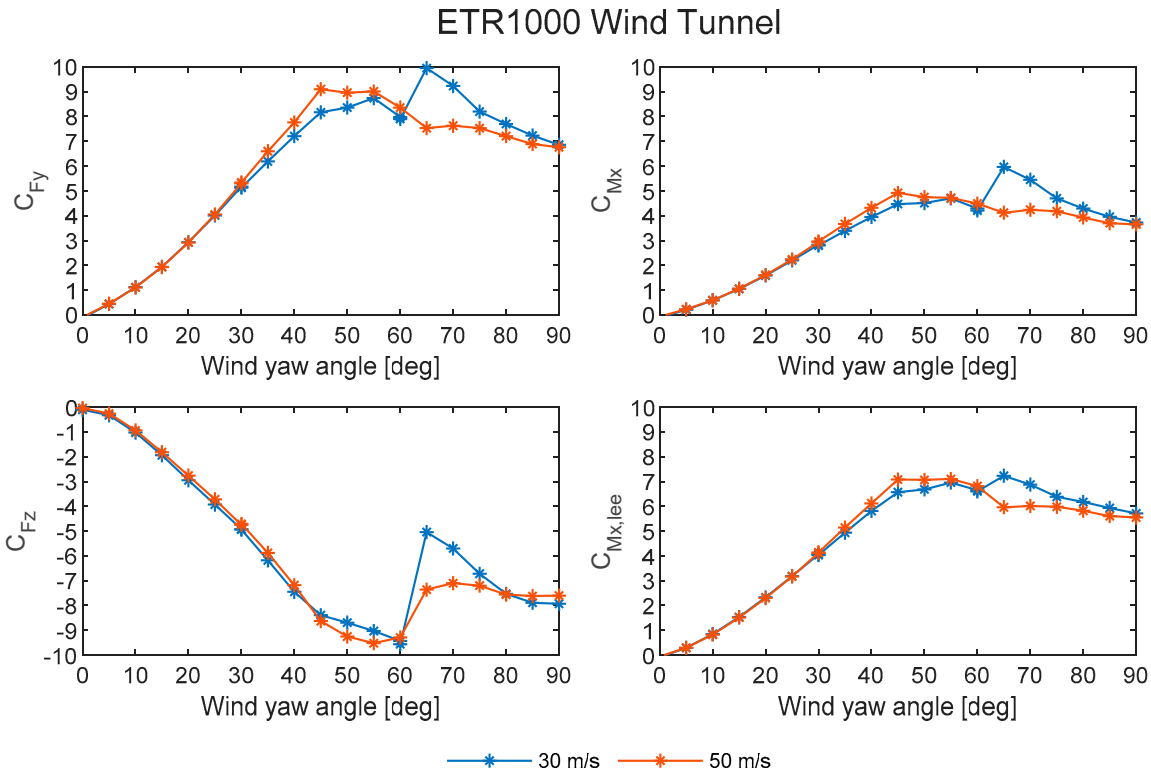

Figure 6. Aerodynamic force coefficients as a function of yaw angle. Wind tunnel test: wind speed 30 m/s and 50 m/s; train: ETR1000; scenario: STBR.

Aerodynamic coefficients measured at 30 m/s show a sudden change between 60° and 65°. This variation leads to an increment of lateral force and rolling moment coefficients, while lift force coefficient decreases. Consequently, the effect on the lee-rail rolling moment coefficient, that is a combination of rolling moment and lift force, is lower in magnitude, although it is still clearly observable.

On the contrary, all the aerodynamic coefficients measured in the wind tunnel at 50 m/s of wind speed do not show this abrupt change: they reach a maximum between 45° and 55° and then decrease, with an almost monotonous trend, up to 90°.

3.2. Pressure Distribution

Mean pressure distributions on the surface of the train for all the eleven tapping loops are presented in Figure 6. The results correspond to the wind tunnel test with wind yaw angle of 65°, being the angle at which the biggest difference in force aerodynamic coefficients is observed.

At 65°, for tapping loops 1–5, no significant differences are observed between the results at 30 m/s and 50 m/s. The pressure distribution shows a positive pressure on the windward side and a uniform suction around the upper part and leeward side of the train nose. The presence of a sharp edge on the upper windward corner of the nose locks up the flow separation point, whose position is independent of the wind speed.

On the contrary, for tapping loops 6 to 8, two different flow distributions depending on the wind speed may be observed. For the wind speed equal to 30 m/s, the behaviour of the flow is in line with the behaviour found for sections 1 to 5: the flow over the roof separates early, and thus a uniform pressure distribution is observed on the roof and on the leeward side of the train body. On the contrary, when the wind speed is 50 m/s, the flow remains attached to the roof and a large suction peak over the windward roof corner is observed.

Pressure coefficient in tapping loops 9, 10 and 11 have a similar behaviour for both wind speeds, but the suction zone in the windward corner of the roof is smaller and less pronounced for the test at 30 m/s.

The uniform pressure distribution observed around the whole roof zone when wind speed is set to 30 m/s, typical of a completely separated flow over the roof, is consistent with the important reduction in lift force observed from the corresponding coefficient. On the contrary, the typical suction peak, observed at the windward corner of the roof zone in the central portion of the car body leads to an increase in the lift, as shown in Figure 6. Moreover, the suction zone over windward corner of the roof, not only increases lift, but also reduces side force.

As outlined by pressure distributions displayed in Figure 7, the gaps observed over 65° in force aerodynamic coefficients at two wind speeds, are mainly due to the different behaviour of the flow at the windward roof corner, in correspondence of the region just behind the train nose (sections 6, 7 and 8), where the roof profile is completely rounded.

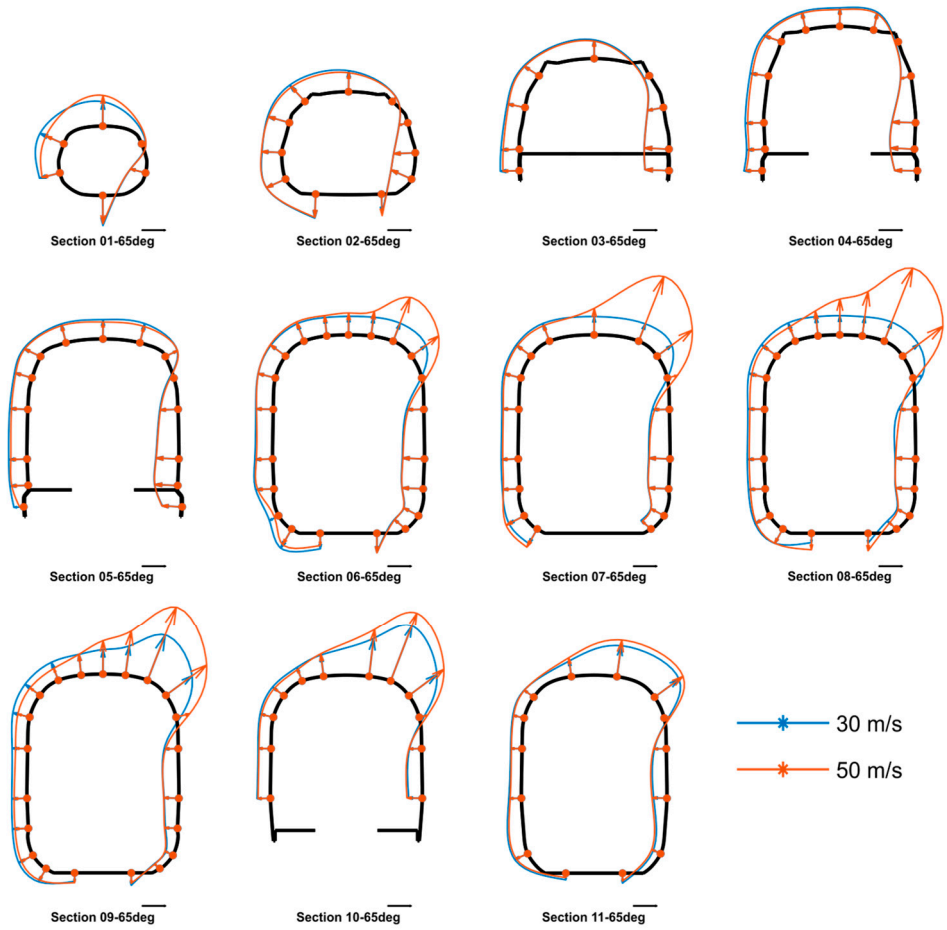

Figure 7. Pressure coefficient around the surface of the train. Wind tunnel test: wind speed 30 m/s and 50 m/s; wind yaw angle = 65°; train: ETR1000; scenario: STBR.

To verify the behaviour at 90°, Figure 8 shows the pressure coefficient around sections 6, 7, and 8 obtained for a wind tunnel test with wind yaw angle set to 90°: it is possible to see that at this angle, the pressure distributions obtained at the two velocities are equivalent. A small difference on the magnitude of the suction zone over the roof is observed for tapping loop 6, that can be responsible for the very small difference in vertical force observed in Figure 6.

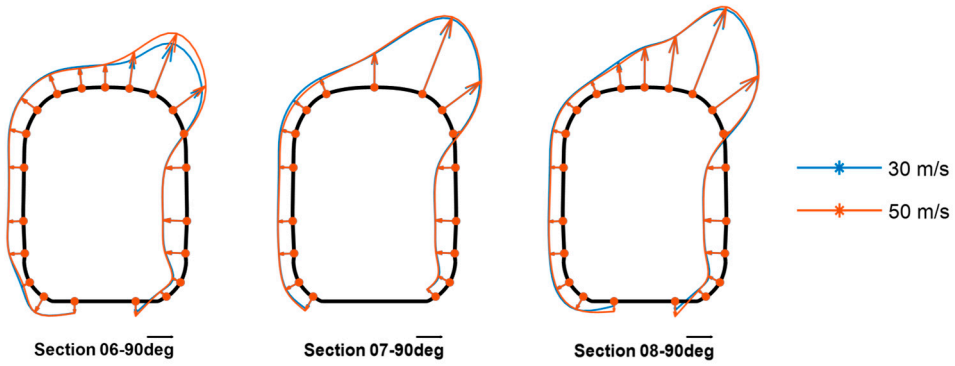

Figure 8. Pressure coefficient around the surface of the train. Wind tunnel test: wind speed 30 m/s and 50 m/s; wind yaw angle = 90°; train: ETR1000; scenario: STBR.

In conclusion, it is interesting to note that the double trend found in the force aerodynamic coefficients over 65° is to be attributed to a different behaviour of the flow and, correspondingly, of the position of the separation point, which, however, occurs only in a well-defined portion of the carriage, i.e., just after the nose, where the roof profile is completely rounded.

In the opinion of the authors, the double trend found in the force aerodynamic coefficients is not only due to the Reynolds number, because the gap between the two trends is not constant in the range 65°–90° (although in this range the car behaves as a bluff body) and because differences in the pressure distribution take place only in some portions of the train. The reason for the appearance of the double trend is a combination of Reynolds number effect, which characterises the fluid-dynamic behaviour of the object, and the geometry of the vehicle, especially due to the particular combination of smooth rounded roof with a train nose characterised of sharp edges, that influences the flow separation location.

Finally, it is interesting to note that, even if, for high-speed trains, a relative wind yaw angle of 65° is difficult to reach because of the big longitudinal component derived from the velocity of the train, the same consideration is not true for conventional trains. Recent studies demonstrated that critical wind speeds that lead high-speed trains to overturning are almost the same as those found for conventional trains [17]. In fact, modern conventional trains are, nowadays, adopting solutions as weight reduction, more aerodynamic nose shapes and smooth rounded roofs, in order to reduce drag and improve efficiency. For these trains, having maximum vehicle speed lower than 200 km/h, the corresponding critical yaw angles are ranged between 40° and 70° [14]. It is then clear how an error in the estimation of the coefficients at these angles can lead to a wrong evaluation when assessing crosswind stability.

4. Conclusions

Wind tunnel tests on a 1:15 scaled ETR1000 model was carried out at different wind speeds.

Over 65° of yaw angles, it was observed that the particular combination of train shape and wind speed causes the occurrence of two different trends in the force aerodynamic coefficients, associated to a different position of the separation line.

These findings highlight that differences can be found on the aerodynamic coefficients, especially at high yaw angles, for some train geometries, i.e., smooth rounded roof, even if tests are made in agreement with the requirements imposed by regulations (European Standard).

The double trend found in the coefficients can have even more important effects for conventional trains with smooth rounded roof because they are more susceptible to work at high relative wind yaw angles due to lower train speed.

It will be interesting to get deep in the analysis by means of CFD computations, in order to better understand the phenomenon and to compare the flow simulated in the wind tunnel with what found at full scale.

Author Contributions: Methodology, E.B.; writing—original draft preparation, C.E.A.R.; writing—review and editing, E.B. and G.T.; supervision, G.T. All authors have read and agreed to the published version of the manuscript.

Funding: This research received no external funding.

Data Availability Statement: Not applicable.

Conflicts of Interest: The authors declare no conflict of interest.

References

1. Sanquer, S.; Barré, C.; Dufresne de Virel, M.; Cléon, L. Effect of cross winds on high-speed trains: Development of a new experimental methodology. *J. Wind. Eng. Ind. Aerodyn.* **2004**, *92*, 535–545. [CrossRef]
2. Ding, Y.; Sterling, M.; Baker, C.J. An alternative approach to modelling train stability in high cross winds. *Proc. Inst. Mech. Eng. Part F J. Rail Rapid Transit* **2008**, *222*, 85–97. [CrossRef]
3. Baker, C.J. The simulation of unsteady aerodynamic cross wind forces on trains. *J. Wind Eng. Ind. Aerodyn.* **2010**, *98*, 88–99. [CrossRef]
4. Cheli, F.; Corradi, R.; Tomasini, G. Crosswind action on rail vehicles: A methodology for the estimation of the characteristic wind curves. *J. Wind. Eng. Ind. Aerodyn.* **2012**, *104–106*, 248–255. [CrossRef]
5. Song, Y.; Zhang, M.; Øiseth, O.; Rønnquist, A. Wind deflection analysis of railway catenary under crosswind based on nonlinear finite element model and wind tunnel test. *Mech. Mach. Theory* **2022**, *168*, 104608. [CrossRef]
6. He, X.; Zou, S. Advances in wind tunnel experimental investigations of train–bridge systems. *Tunn. Undergr. Space Technol.* **2021**, *118*, 104157. [CrossRef]
7. LOC&PAS, TSI RST. Technical specification for interoperability relating to the 'rolling stock–locomotives and passenger rolling stock' subsystem of the rail system in the entire European Union. *Official Journal of the European Union L* **2014**, *356*, 228–393.
8. *EN 14067-6:2018*; Railway Applications—Aerodynamics, Part 6: Requirements and Test Procedures for Cross Wind Assessment. CEN, European Committee for Standardization: Brussels, Belgium, 2018.
9. Baker, C.J.; Jones, J.; Lopez-Calleja, F. Measurements of the cross wind forces on Mark 3 and Class 390 vehicles. In Proceedings of the World Congress on Railway Research, Edinburgh, UK, 28 September–1 October 2003.
10. Baker, C.J.; Jones, J.; Lopez-Calleja, F.; Munday, J. Measurements of the cross wind forces on trains. *J. Wind. Eng. Ind. Aerodyn.* **2004**, *92*, 547–563. [CrossRef]
11. Sun, Z.; Yao, S.; Wei, L.; Yao, Y.; Yang, G. Numerical Investigation on the Influence of the Streamlined Structures of the High-Speed Train's Nose on Aerodynamic Performances. *Appl. Sci.* **2021**, *11*, 784. [CrossRef]
12. Baker, C.J. Ground vehicles in high cross winds part 1: Steady aerodynamic forces. *J. Fluids Struct.* **1991**, *5*, 69–90. [CrossRef]
13. Bocciolone, M.; Cheli, F.; Corradi, R.; Muggiasca, S.; Tomasini, G. Crosswind action on rail vehicles: Wind tunnel experimental analyses. *J. Wind Eng. Ind. Aerodyn.* **2008**, *96*, 584–610. [CrossRef]
14. Giappino, S.; Rocchi, D.; Schito, P.; Tomasini, G. Cross wind and rollover risk on lightweight railway vehicles. *J. Wind Eng. Ind. Aerodyn.* **2016**, *153*, 106–112. [CrossRef]
15. Robinson, C.G.; Baker, C.J. The effect of atmospheric turbulence on trains. *J. Wind Eng. Ind. Aerodyn.* **1990**, *34*, 251–272. [CrossRef]
16. Liang, H.; Sun, Y.; Li, T.; Zhang, J. Influence of Marshalling Length on Aerodynamic Characteristics of Urban Emus under Crosswind. *J. Appl. Fluid Mech.* **2023**, *16*, 9–20. [CrossRef]
17. Araya, R.C.E.; Baratelli, E.; Rocchi, D.; Tomasini, G.; Iraeta, S.M.; Artano, M. Aerodynamic Effects of Different Car Body Configurations in a Conventional Train under Crosswinds. In Proceedings of the Fifth International Conference on Railway Technology: Research, Development and Maintenance, Montpellier, France, 22–25 August 2022.